JOURNAL OF CATALYSIS 84, 189–199 (1983)

Preparation and Properties of Raney Nickel–Cobalt Catalysts

J. P. ORCHARD, A. D. TOMSETT, M. S. WAINWRIGHT,* AND D. J. YOUNG

School of Chemical Engineering and Industrial Chemistry, The University of New South Wales, P.O. Box 1, Kensington, New South Wales, 2033 Australia

Received April 12, 1983; revised June 21, 1983

The leaching behavior in aqueous NaOH of Al–Co–Ni alloys containing 50 wt% Al and approximately 0, 10, 20, 30, 40, and 50 wt% Co has been examined. The alloys were partially leached and the product was examined metallographically. All of the alloys leached rapidly, with the relative reactivity of the phases in the nickel–aluminum alloy being Al(Ni) > $NiAl_3$ > Ni_2Al_3. All cobalt–aluminum phases were found to leach rapidly to completion. Catalysts prepared from the Al–Co–Ni alloys were characterized by physical adsorption, chemisorption, and temperature-programmed desorption experiments. The H_2 evolved in the TPD tests decreased with cobalt addition and seems related to the Ni part of the catalyst. Studies of the hydrogenation of cyclohexene and adiponitrile at 25°C and 101 kPa were used to evaluate catalyst activities. The rates of hydrogenation of both compounds increased in the order cobalt ≤ nickel–cobalt < nickel.

INTRODUCTION

The activity and selectivity of Raney nickel hydrogenation catalysts can generally be improved by the addition of small amounts of a promoter metal, usually one of the transition elements. Montgomery (*1*) studied the effects of the addition of up to 10 wt% of Co, Cr, Cu, Fe, and Mo to Raney nickel in the hydrogenation of nitrile, carbonyl, nitro, and olefinic compounds. His results showed that the effectiveness of promoters varies markedly for the type of metal and unsaturated organic compound. Other studies of cobalt-promoted Raney catalysts have also been concerned with measuring activities for various hydrogenation reactions including Fischer–Tropsch synthesis (*2*), unsaturated organic compounds (*3*) and substrates such as cyclohexene, nitrobenzene, phenol, and acetone (*4*). These studies included little or no characterization of the surface and pore structure of the catalysts containing promoters. In none of the studies was any attempt made to follow the extent or rate of leaching.

In a previous study (*5*) we used metallography, X-ray diffraction, and electron microprobe analysis to provide information on the leachability of Al–Cu–Ni alloys containing 50 wt% aluminum. We also used physisorption, chemisorption, and thermal desorption measurements to determine the surface properties of those catalysts (*6*). The present paper provides new information on the leachability of six Al–Co–Ni alloys in which the Co/Ni ratio is continuously varied. We have also used adsorption and desorption measurements to determine the nature of the H_2 stored in catalysts prepared from these alloys and the influence that it has in determining the activities of the catalysts for the hydrogenation of cyclohexene and adiponitrile. The promotional effects of small amounts of Ni in Raney cobalt and Co in Raney nickel were measured in a study of catalysts prepared from alloys containing less than 6 wt% of the promoting metal.

METHODS

Catalyst preparation. Samples of all the alloys listed in Table 1 were obtained as approximately 8-mm pieces from the Davison Chemical Division of the W.R. Grace Company. These were crushed and screened to provide particles less than 100-

0021-9517/83 $3.00

TABLE 1

Compositions and Extent of Leaching of Alloys

Sample	Alloy (wt%)			Catalyst (wt%)				Al Extraction (%)	
	Ni	Co	Al	Ni	Co	Al	$Al_2O_3 \cdot 3H_2O$	H_2 Evolution	AAS Analysis
1	49.6	—	50.7	82.5	—	11.4	9.3	82.1	90.3
2	51.7	2.2	47.2	73.5	4.3	16.1	9.3	82.3	81.1
3	48.5	4.5	47.2	71.9	7.6	15.6	7.5	82.0	81.6
4	43.8	6.1	46.2	68.8	9.4	16.0	8.9	82.0	82.2
5	42.6	10.1	48.5	63.8	14.2	14.6	11.3	84.2	85.1
6	31.6	19.7	47.9	50.8	33.5	9.1	10.1	92.1	92.9
7	21.0	30.0	47.0	34.5	51.0	8.5	9.2	95.3	93.3
8	10.1	38.5	51.7	16.7	69.7	7.4	9.5	89.9	95.4
9	4.4	49.6	47.9	6.7	78.0	9.6	8.7	97.7	92.4
10	3.8	48.3	51.1	4.2	83.2	9.1	5.4	92.9	91.6
11	—	48.8	51.3	—	91.2	4.6	6.4	95.9	97.5

μm diameter for most of the characterization methods.

The catalysts were prepared using an extraction method similar to that reported by Freel and co-workers (*7*). A 40% aqueous solution of NaOH was added to the (100 μm) alloy particles over a period of 2.5 h. The total amount of caustic added was calculated on the basis of a threefold excess over the amount required to completely react with the aluminum in the alloy samples. After completion of the extraction reaction (monitored as hydrogen evolution using a wet test gas meter) the catalysts was washed in distilled water until the pH of the wash water was 7. The catalysts were stored under distilled water prior to use. The extent of extraction was measured by both hydrogen evolution and chemical analysis by dissolving the catalysts in acid and analyzing by atomic absorption spectroscopy.

The composition of the catalysts presented in Table 1 were estimated by the procedure described by Robertson and Anderson (*15*). The catalysts were assumed to contain only metallic nickel, cobalt, aluminum, and alumina trihydrate. The difference between the total mass and the sum of the masses of total nickel (and/or cobalt) and total aluminum was taken as the $O_3 \cdot 3H_2O$ component of the alumina trihydrate.

Morphological investigation. To examine the reaction rim microscopically, partially extracted alloy pieces were vacuum-impregnated with a cold-setting resin, cross-sectioned and metallographically polished to a 1-μm finish. Under an optical microscope the reaction rim was clearly visible, and representative areas were chosen for the micrographs.

Phase identification. Both the unreacted alloy and the reaction rim were analyzed with an electron microprobe in order to discover both the identity of the phases in each alloy and their behavior under leaching conditions. Point counts over a 20-s period were obtained from the microprobe. These were calibrated using CoAl and pure Ni standards. Systematic corrections were applied to the data for atomic number, mass absorption, and fluorescence effects.

The microprobe investigation was complemented by powder X-ray diffraction. The original alloys were crushed and ground to 40 μm diameter and examined in the usual fashion. The pyrophoric nature of the material after extraction mean that it was necessary to coat the powdered catalysts with collodion prior to examination. Cu$K\alpha$ radiation was used and the diffraction patterns were compared with those on

ASTM files to obtain the identity of the phases present.

Estimates of the catalyst crystallite size were obtained from X-ray line broadening using the Scherrer equation. Warren's relationship (*8*) using KCl as the standard, was used to correct for instrumental line broadening.

Adsorption measurements. BET surface areas were obtained from the adsorption of nitrogen at −195°C, using a Micromeritics 2100E ORR surface area, pore volume analyzer. Samples were transferred to the adsorption flask under water and evacuated at 130°C overnight. The degassed samples were weighed on completion of each experiment.

The samples for the hydrogen chemisorption studies were also evacuated overnight using the same procedure. The evacuation temperatures used were 150 or 250°C. The chemisorption of hydrogen was determined by measuring isotherms at 25°C in the range 26 to 60 kPa pressure. A time of 1½ h was allowed for equilibration at the first point and 30 min for each subsequent point. The isotherms were linear and showed almost no dependence on hydrogen pressure. The values presented in Table 4 were determined from the isotherms at a pressure of 40 kPa.

Temperature-programmed-desorption studies. The apparatus used for the temperature-programmed desorption (TPD) measurements was similar to that described by Nicolau and Anderson (*9*). Catalysts were transferred to a glass U-tube reactor and evacuated at room temperature for 2 to 3 h. The reactor was then heated at a constant rate of 5°C/min in a tube furnace controlled by a linear temperature programmer (Honeywell Model 7456.3.642.2.01). The desorbed hydrogen was continuously analyzed using a thermal conductivity detector with argon (99.95% purity) as the carrier gas. After analysis the samples were cooled to room temperature and left for 65 h under a flow of high purity (99.99%) hydrogen. The excess hydrogen was then removed by evacuation and the readsorbed hydrogen was analyzed by the procedure described above.

Activity measurements. The activity of each catalyst for the hydrogenation of cyclohexene and adiponitrile was determined. The reactions were carried out in pure hydrogen at 25°C in a vigorously stirred, glass-jacketed reactor using methanol as the solvent. The required mass of catalyst was washed with methanol before being transferred to the reactor. The reaction was followed by observing the rate of change in gas volume at a constant pressure of 1 atm.

RESULTS

Cross sections of reacted alloys are shown in Fig. 1, where it can be seen that each of the alloys developed a rim of reacted material. A sharply defined reaction front was formed in each case. To a first approximation, the thickness of the leached rim was uniform around the sample periphery.

The microprobe results for the reaction product rim yielded mass balances of approximately 70% due to the porous nature of the material. These were scaled up to give a 100% mass balance on the assumption that the effect of porosity on the generation and emergence of X rays is independent of the nature of the element.

A series of microprobe analyses showed that no net concentration gradient exists across the leached rim and that, within the spatial resolution of the microprobe (ca. 2 μm), a discontinuous change in chemical composition occurs at the alloy/rim interface. The composition of the rim was nonuniform, there being regions of at least two distinctly different but homogeneous chemical composition in each case. The sizes and shapes of these regions corresponded to the microstructural parameters of the parent alloy. Analyses of these leach reaction products are summarized in Table 2 together with the chemical compositions of the alloy phases.

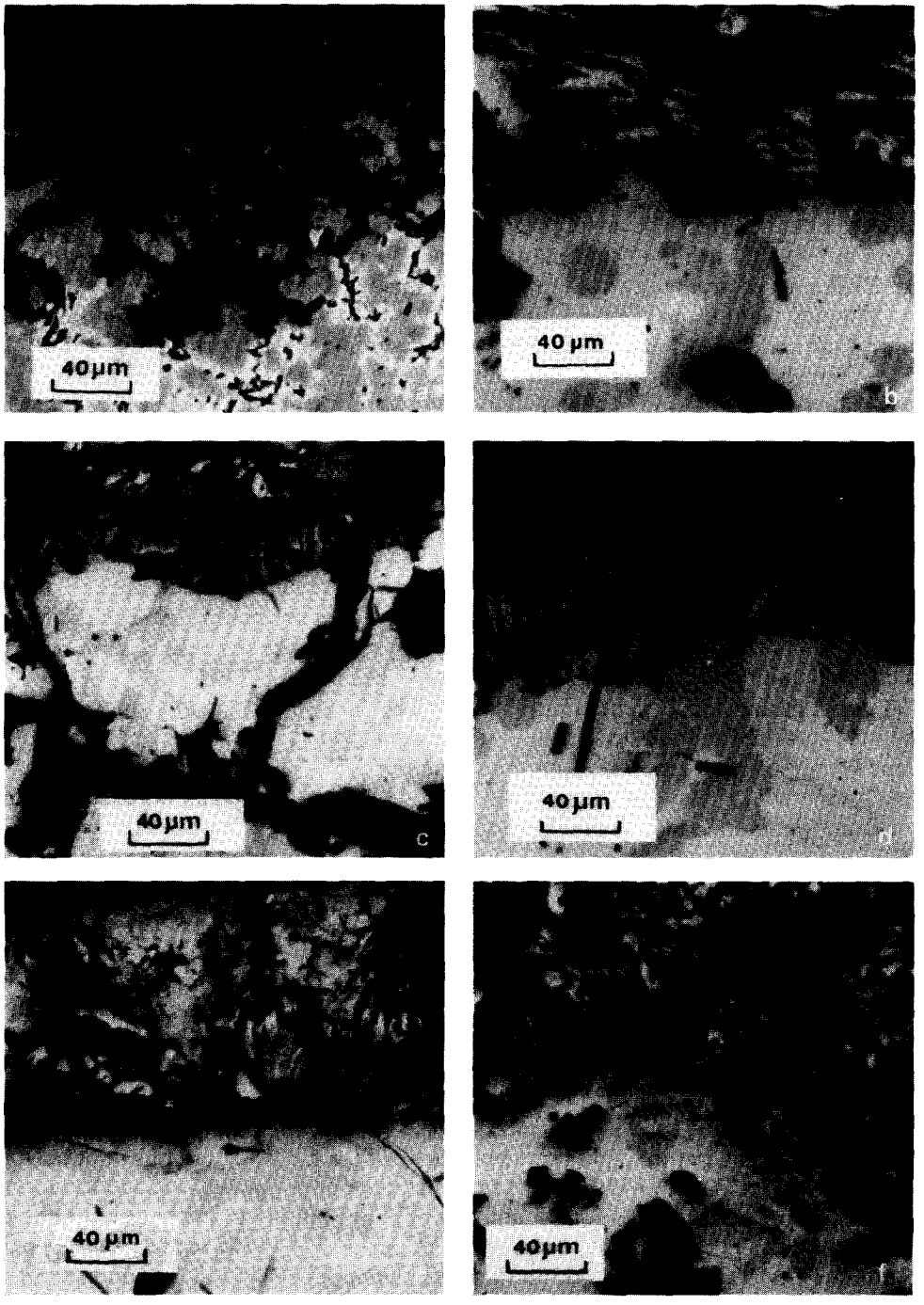

FIG. 1. Micrographs of cross sections through partially leached alloys: (a) Al–50Ni; (b) Al–43Ni–10Co; (c) Al–32Ni–20Co; (d) Al–21Ni–30Co; (e) Al–10Ni–39Co; (f) Al–49Co.

TABLE 2

Microprobe Analyses of Alloys and the Resulting Catalysts (atom%)

Sample	Alloy		Catalyst	
	Grey phase	Light phase	Grey area	Dark area
2	$Ni_{39}Co_1Al_{59}$	$Ni_{26}Co_1Al_{73}$	$Ni_{86}Co_3Al_{29}$	$Ni_{82}Co_4Al_{14}$
3	$Ni_{39}Co_3Al_{60}$	$Ni_{24}Co_3Al_{73}$	$Ni_{64}Co_5Al_{31}$	$Ni_{77}Co_9Al_{14}$
4	$Ni_{37}Co_3Al_{60}$	$Ni_{24}Co_3Al_{73}$	$Ni_{62}Co_8Al_{30}$	$Ni_{71}Co_{10}Al_{19}$
5	$Ni_{32}Co_8Al_{60}$	$Ni_{20}Co_9Al_{71}$	$Ni_{60}Co_{14}Al_{26}$	$Ni_{61}Co_{27}Al_{12}$
6	$Ni_{25}Co_{18}Al_{57}$	$Ni_{17}Co_{15}Al_{68}$	$Ni_{38}Co_{27}Al_{35}$	$Ni_{47}Co_{43}Al_{10}$
7	$Ni_{(20-15)}Co_{(25-29)}Al_{55}$	$Ni_{12}Co_{20}Al_{68}$	$Ni_{35}Co_{33}Al_{32}$ + $Ni_{30}Co_{41}Al_{29}$	$Ni_{34}Co_{60}Al_6$
8	$Ni_8Co_{40}Al_{52}$	$Ni_5Co_{27}Al_{68}$	$Ni_9Co_{40}Al_{51}$	$Ni_{14}Co_{77}Al_9$
9	$Ni_3Co_{46}Al_{51}$	$Ni_1Co_{29}Al_{70}$	$Ni_3Co_{46}Al_{51}$	$Ni_4Co_{88}Al_8$
10	$Ni_2Co_{46}Al_{52}$	$Ni_1Co_{29}Al_{70}$	$Ni_2Co_{46}Al_{52}$	$Ni_4Co_{88}Al_8$
11	$Co_{49}Al_{51}$	$Co_{31}Al_{69}$	$Co_{49}Al_{51}$	$Co_{94}Al_6$

The results of the X-ray diffraction investigation of the alloy samples are shown in Table 3. Diffraction patterns obtained from the catalysts consisted of lines which were so broad that nickel and cobalt could not be distinguished. Crystallite sizes calculated from the line broadening are also shown in Table 3, the calculations being made on the basis that the single peak observed corresponded to the element present in greatest excess in the catalyst.

Adsorption/Desorption Studies

The surface areas calculated from the simple BET equation and hydrogen chemisorption data are presented in Table 4. The chemisorption data for catalysts evacuated at 150°C have been normalized to surface area by dividing the volume chemisorbed by the monolayer volume, V_m, calculated from the nitrogen isotherm.

Pore volumes and mean pore radii, calculated from the complete physical adsorption isotherms for catalyst samples 1, 5–8, and 11 are presented in Table 5. The pore volume, V_s, was estimated from the amount of nitrogen adsorbed at a relative pressure of 0.99 calculated as normal liquid. The "average" pore radius, r_a, was calculated by the equation for nonintersecting cylin-

TABLE 3

X-Ray Diffraction Analyses of Selected Alloys and Metal Crystallite Sizes of the Fully Extracted Catalysts

Alloy	Phases present	Catalyst crystallite size (Å)
1	Ni_2Al_3, $NiAl_3$, Al	51
5	Ni_2Al_3, (Co_2Al_5 + $NiAl_3$)[a]	38
6	Ni_2Al_3, (Co_2Al_5 + $NiAl_3$)[a]	46
7	Co_2Al_5, CoAl, Ni_2Al_3	51
8	Co_2Al_5, CoAl, Ni_2Al_3	52
11	Co_2Al_5, CoAl	47

[a] Presence of ternary phase cannot be excluded.

TABLE 4

Surface Areas and H_2 Chemisorption on Raney Ni–Co Catalysts

Sample	V_m (cm³ STP/g)	Surface area (m²/g)	Chemisorbed gas (cm³ STP/g)		$V_{H_2}^{150}/V_m$
			$V_{H_2}^{150}$	$V_{H_2}^{250}$	
1	13.30	58.1	15.8	13.0	1.19
2	17.46	76.3	12.9	10.7	0.74
3	21.01	91.8	13.1	10.3	0.62
4	19.89	86.9	11.0	9.6	0.55
5	13.62	59.5	10.7	8.6	0.78
6	10.48	45.8	8.0	5.5	0.76
7	12.40	54.2	8.4	5.5	0.68
8	11.51	50.3	10.6	6.8	0.92
9	7.87	34.3	7.4	5.1	0.94
10	6.06	26.5	6.1	3.8	1.01
11	6.11	26.7	5.1	3.9	0.83

TABLE 5

Pore Volumes and Pore Radii of Catalysts

Sample	Pore volume ($cm^3\ g^{-1}$)	Pore radius (Å)	
		r_p	r_a
1	0.068	25	24
5	0.124	20–70	42
6	0.068	20	30
7	0.084	28	31
8	0.074	19	30
11	0.056	24–100	42

drical pores, $r_a = 2V_s/S_{BET}$ (*10*). The values of r_p correspond to maxima in plots of $\Delta V_p/\Delta r_p$ versus r_p.

The effects of evacuation temperature on the surface area of the catalysts are given in Table 6. Mean crystallite sizes are also given for Raney nickel. The crystallite size of the Raney cobalt samples could not be measured after heating under vacuum as the diffraction peaks were obscured by instrument noise.

The total volumes of hydrogen evolved from the fresh catalysts and of hydrogen readsorbed after the thermal desorption are shown in Table 7. Typical TPD curves for the catalysts are presented in Fig. 2. The peak at 86°C was assumed to be due to the presence of water in the catalyst that reacted with residual aluminum, as suggested by Nicolau and Anderson (*9*) and was disregarded in the calculation of hydrogen evolution.

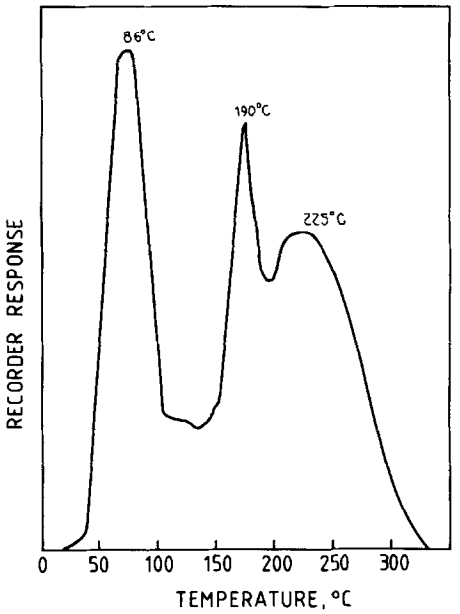

FIG. 2. Typical TPD curve sample 6.

The TPD spectra of all six catalysts studied had peaks at about 190 and 224°C although the relative amounts of hydrogen associated with each peak varied. A third peak occurred in three of the catalysts, at

TABLE 6

Surface Area and Crystallite Size of Catalysts after Evacuation under Various Conditions

Sample	Evacuation temp. (°C)	Surface area (m^2/g)	Crystallite size (Å)
1	150	62.6	77
	250	51.1	77
	None	—	51
	50	103.3	—
	150	69.3	—
	250	55.7	—
6	150	41.3	—
	250	79.6	—
	250	69.2	—
11	150	17.1	—
	250	61.5	—
	150	22.6	—
	250	28.3	—

TABLE 7

Temperature-Programmed Desorption Data

Sample	Hydrogen evolved [cm^3 (STP)/g]	Error	Readsorbed hydrogen [cm^3 (STP)/g]
1	34.1	3.07	9.4
5	22.0	1.23	5.8
6	22.0	0.83	3.0
7	12.0	0.38	3.3
8	8.4	0.77	3.5
11	3.8	0.34	1.2

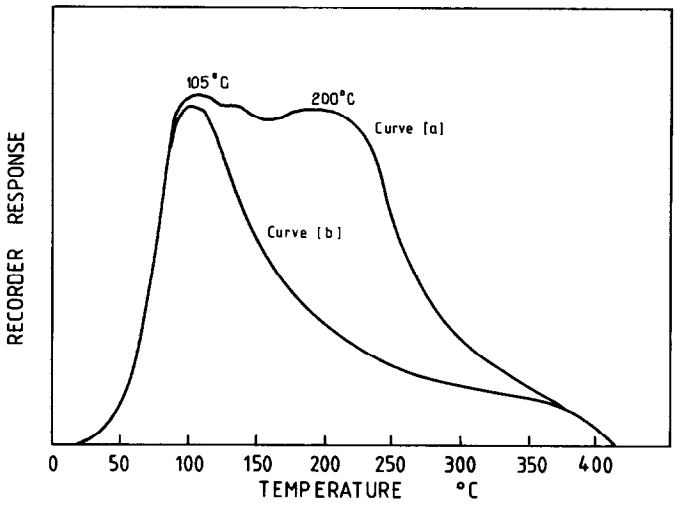

FIG. 3. Typical TPD curves after readsorption of hydrogen. Curve (a) sample 1. Curve (b) samples 5, 6, 7, 8, 11.

approximately 150°C in catalysts 1 and 5 and at 270°C in catalyst 11.

TPD curves for the readsorbed hydrogen are given in Fig. 3. They indicate that Raney nickel evolved hydrogen at a constant rate between 105 and 200°C, while the other five catalysts studied did not show this continued evolution above 105°C.

The first-order hydrogenation rate constants per gram of catalyst and per unit total surface area of the catalyst for both reactions studied are given in Table 8.

DISCUSSION

Alloy Structures

It appears from Fig. 1 that each of the alloys consists of two major phases. Micrographs (not shown) of the alloys containing less than 10% nickel were similar in appearance to that of the alloy containing no

TABLE 8

Activity Data for Raney Ni–Co Catalysts

Sample	Cyclohexene		Adiponitrile	
	Rate $(min^{-1} g^{-1}) \times 10$	Rate $(min^{-1} g^{-1}) \times 10^3$	Rate $(min^{-1} g^{-1}) \times 10^2$	Rate $(min^{-1} g^{-1}) \times 10^4$
1	3.45	5.94	2.65	4.56
2	1.56	2.04	2.59	3.39
3	2.49	2.71	2.82	3.07
4	2.59	2.98	3.17	3.65
5	3.50	5.88	2.46	4.13
6	2.03	4.43	1.66	3.62
7	1.93	3.56	1.40	2.58
8	1.46	2.90	0.97	1.93
9	0.47	1.37	0.32	0.930
10	0.099	0.374	0.24	0.906
11	0.039	0.146	<0.005	<0.02

nickel. Similarly, alloys containing less than 10% cobalt had the same microstructure as the alloy containing no cobalt.

Microprobe and X-ray diffraction data (Tables 2 and 3) for alloys containing up to 20% nickel show that the major phases are (Co,Ni)Al and $(Co,Ni)_2Al_5$. The significant solubility of nickel in these cobalt based phases is to be expected in view of the close similarity of the elements. Alloys containing more than 20% nickel all contain $(Ni,Co)_2Al_3$ but none of the (Co,Ni)Al phase. The identity of the second major phase is not entirely clear except in the case of alloys containing less than 10% cobalt, where the phase is $(Ni,Co)Al_3$. In alloys containing 10 and 20% cobalt the second phase has a microprobe analysis intermediate to the $(Ni,Co)Al_3$ and $(Co,Ni)_2Al_5$ phases. The X-ray diffraction patterns can be satisfactorily interpreted as corresponding to a mixture of $NiAl_3$ and Co_2Al_5 (plus Ni_2Al_3). However, these phases could not be resolved optically or with the electron microprobe. In the absence of a Ni–Co–Al ternary phase diagram it is not possible, from the evidence to hand, to distinguish between the possibilities of an intimately associated two-phase mixture and a ternary phase of appropriate composition but unknown crystal structure.

In the Ni–Al system the phases found are $NiAl_3$ and Ni_2Al_3; NiAl is known but is usually not found in Raney alloys. For the Co–Al system, Co_2Al_5 and CoAl are the phases usually found.

Morphology of Leaching

Examination of Fig. 1 and of the microprobe results in Table 2 reveals the appearance and chemical composition of the alloys after caustic attack. It is possible from these results to discuss the behavior of each phase after leaching.

Results for alloys containing less than 10% cobalt showed that the phase $NiAl_3$ leaches considerably faster than Ni_2Al_3. From the fact that the areas of leached Ni_2Al_3 do not appear to have a marked concentration gradient, it can be said that this phase not only leaches more slowly, but when fully leached, still contains approximately 30 atom% aluminum. The hydrogen evolution data in Table 1 which shows that only 82% of the theoretical volume was evolved indicates that this is aluminum which does not leach under the extraction conditions used.

The intermediate group of alloys (10 and 20% cobalt) contained the slow leaching Ni_2Al_3 and a phase whose behavior under caustic attack was similar to both $NiAl_3$ and Co_2Al_5. Thus the leachability of the alloy is not helpful in elucidating the composition of these two alloys. Alloys containing 30% or more cobalt all had Co_2Al_5 as a major phase and this phase was observed to leach rapidly.

The cobalt rich alloys (cobalt $\geq$ 30%) show behavior similar to the nickel rich alloys in that both groups contain a fast leaching phase and one that leaches more slowly. In this case Co_2Al_5 leaches rapidly while CoAl reacts more slowly. There is a major difference, however, between CoAl and the slow leaching Ni_2Al_3; this is that while CoAl is even slower to react than Ni_2Al_3 it will eventually react to lose almost all its aluminum content. This is evidenced by the fact that the actual H_2 evolution for these alloys is 99% of the theoretical value.

It is apparent from Fig. 1 that the microstructure of the alloys are reproduced in the product catalysts. From Table 2 it is seen that the nickel to cobalt ratios in the catalyst regions are essentially the same as in their precursor alloy phases. Both observations indicate that the mechanism of leaching is one of selective dissolution rather than dissolution–reprecipitation.

Physical and Chemical Adsorption Measurements

The addition of up to 10% cobalt to the Raney nickel alloy was found to increase the surface area of the catalyst. However, cobalt additions greater than 10% decreased the surface area. The surface areas

obtained for catalysts 1–5 and 11 are in good agreement with those reported in the literature (*7, 11, 12, 13*).

The decrease in surface area accompanying the increase in alloy cobalt content above 10% may be attributed to the disappearance of the $NiAl_3$ phase. This phase is known (*7*) to contribute a much higher pore volume and significantly higher surface area when leached, than does Ni_2Al_3. The observed increase in surface area as the alloy cobalt concentration increases from zero to 10% must be due either to an alteration of the phase volume fractions in the alloy or to a change in leaching behavior of the individual phases. Present measurements do not permit a distinction to be drawn between the two possibilities.

The volume of hydrogen chemisorbed decreases with increasing cobalt content except for catalysts 6–8 where there is a slight increase with increasing cobalt content, although the volume is still significantly lower than the results obtained for Raney nickel. This minimum in chemisorbed hydrogen at catalyst 6 corresponds to the point where the phases present in the original alloy change from being predominantly Ni–Al to Co–Al phases. Alloys 7 and 8 contain Co_2Al_5 and CoAl in addition to Ni_2Al_3 suggesting that the leach residues of the cobalt-based phases are of higher surface area than those of the secondary phases in alloys 5 and 6. The drop in surface area observed when Ni_2Al_3 vanishes at still higher cobalt levels, indicates that this phase produces a leach residue of still higher surface area.

The BET surface areas obtained at different evacuation temperatures (Table 6) indicate that the evacuation temperature is critical in comparing surface areas of Raney catalysts. The behavior of Raney nickel differed from that of Raney cobalt and an intermediate catalyst when evacuated at different temperatures. The surface area of Raney nickel decreased and the nickel crystallite size increased with increasing evacuation temperature, while for the other two catalysts studied the surface area increased with an increase in evacuation temperature from 150 to 250°C. The results obtained for Raney nickel agree with those obtained by Mars *et al.* (*14*) and Freel *et al.* (*7*) for a catalyst having a high alumina content and Robertson and Anderson (*15*). These results indicate that some rearrangement of the catalyst surface occurs during evacuation. This also explains the decrease in the volume of chemisorbed hydrogen with increasing evacuation temperature. Thus the ratio of $V_{H_2}^{150}/V_{H_2}^{250}$ is almost the same as the ratio at V_m^{150}/V_m^{250} for Raney nickel.

The increase in surface area obtained for the other two catalysts is due to the presence of bayerite (*15, 16*) in the catalyst. Lippens and De Boer (*17*) have found that the surface area of bayerite increases from 5 m^2/g when evacuated at 120°C to 489 m^2/g when evacuated at 250°C. This also indicates that catalysts containing cobalt have higher stability than Raney nickel at temperatures above 150°C.

Temperature-Programmed Desorption Studies

The value of 34 cm^3 (STP)/g of hydrogen obtained as the hydrogen content for Raney nickel compares well with the value of 25 cm^3 (STP)/g obtained by Nicolau and Anderson (*9*) when the differences in catalysts preparation techniques are taken into account. As can be seen from Table 7 the addition of cobalt to the catalyst significantly decreases the hydrogen content of the catalyst. A second effect of the addition of cobalt is to increase the relative amount of hydrogen in the peak at 224°C (Fig. 2). Thus cobalt appears to produce a tendency toward higher temperature evolution.

The presence of the two peaks at 190 and 224°C on all curves indicates that these two forms of hydrogen have bond energies independent of the catalyst composition. While the bond energies seem independent of composition, the amounts of each type of hydrogen are significantly affected.

The peak at 86°C was very much lower in

Raney cobalt than for the other catalysts. This observation is consistent with the view of Nicolau and Anderson (*9*) that this peak is due to the reaction of water with the residual aluminum in the catalyst. The aluminum extraction results (Table 1) indicate that the 50% cobalt–50% aluminum was leached to a much greater extent than the other alloys. Thus the lower peak can be explained by postulating that the aluminum has become the limiting reagent in the reaction with water and this prevents Raney cobalt from producing a peak at 86°C similar in height to those of the other catalysts.

The TPD curves after readsorption in Fig. 3 show for all catalysts except Raney nickel a single peak, indicating that the hydrogen originated from one source only. As the readsorption procedure was such that chemisorption would have occurred, it is reasonable to interpret the peak as corresponding to hydrogen chemisorbed onto the catalyst.

The shape of the curve for Raney nickel, which showed relatively constant hydrogen evolution between 105 and 200°C, can be explained in terms of the heating rate used. As desorption is an activated process, a rapid heating rate can result in the hydrogen evolution lagging behind the temperature range. As Raney nickel evolved more hydrogen than the other catalysts, it would be the most susceptible to a lag of this nature. Thus the hydrogen evolution between 105 and 200°C can be interpreted as being the result of the heating rate rather than a property of the catalyst.

As chemisorbed hydrogen is evolved at 105°C on both Raney nickel and cobalt, a peak at this temperature might have been expected in the TPD curves of the fresh catalysts. The absence of a peak at 105°C can be explained in two ways. First, the presence of stored hydrogen may have modified the nature of the chemisorbed hydrogen causing it to be evolved at higher temperatures. The second, and more probable explanation is that the amount of chemisorbed hydrogen on the fresh catalysts is much less than that achieved in the readsorption experiments. The "stored" hydrogen in the fresh catalysts were evolved at higher temperatures which indicates that it was bound more strongly. Thus, hydrogen produced during the extraction may preferentially be contained as "stored" hydrogen rather than chemisorbed hydrogen. This would mean that a low chemisorption peak may have occurred at about 105°C. However, this peak would be masked by the peak produced by residual water at 86°C.

From this, it appears that the TPD measurements carried out on the fresh catalysts reflected the amount and character of the "stored" hydrogen alone and not a composite result of both "stored" and chemisorbed hydrogen.

The volume of hydrogen chemisorbed in these experiments confirm the trends shown in the chemisorption measurements. The volume of hydrogen chemisorbed on the catalysts which had been heated to 450°C was less than that chemisorbed on a catalyst evacuated at 250°C. This decrease in chemisorbed hydrogen suggests that a rearrangement of the metal surface occurs as the evacuation temperature is increased. The surface areas and nickel crystallite sizes in Table 6 also show this effect.

Catalyst Activities

The results in Table 8 show that the activity with respect to cyclohexene decreased with increasing cobalt content. This decrease can be contributed to the reduction of the amount of nickel in the catalyst. The catalysts prepared from alloys containing up to 10% cobalt showed an increase in activity with respect to the hydrogenation of adiponitrile. The addition of more cobalt to the alloys decreased the activity. The catalysts prepared from the alloy containing 6% cobalt gave the highest activity. The results agree with those obtained by Montgomery (*1*) who studied a range of alloys with 0–10% cobalt.

The activity on a surface area basis

shows that Raney nickel had the highest activity for both reactions, thus, the promotional effect of small amounts of cobalt in Raney nickel for the hydrogenation of nitriles may be due to the increase in surface area. The decrease in these data to a minimum at Raney cobalt indicates that Raney cobalt is a much weaker hydrogenation catalysts than Raney nickel.

The hydrogenation activity of the catalysts also appears to be related to hydrogen chemisorbed onto the catalyst. The addition of cobalt to Raney nickel reduces the amount of hydrogen chemisorbed onto the catalyst as well as the activity of the catalyst.

ACKNOWLEDGMENTS

The authors thank S. R. Montgomery of the Davison Chemical Division of W. R. Grace and Company for furnishing the Raney alloys used in this work. The financial assistance of the ARGS is gratefully acknowledged.

REFERENCES

1. Montgomery, S. R., *in* "Catalysis of Organic Reactions" (W. R. Moser, Ed.), pp. 383–409, Dekker, New York, 1981.
2. Fischer, F., and Meyer, K. Ber., **67B**, 253 (1934).
3. Paul, R., *Bull. Soc. Chim. Fr.* **13,** 208 (1946).
4. Ishikawa, J., *Nippon Kagaku Zosshi* **81,** 837, 842, 1179, 1187, 1354, 1489 (1960); **82,** 1, 135 (1961).
5. Young, D. J., Wainwright, M. S., and Anderson, R. B., *J. Catal.* **64,** 116 (1980).
6. Wainwright, M. S., and Anderson, R. B., *J. Catal.* **64,** 124 (1980).
7. Freel, J., Pieters, W. J. M., and Anderson, R. B., *J. Catal.* **14,** 247 (1969).
8. Warren, B. E., *J. Appl. Phys.* **12,** 375 (1941).
9. Nicolau, I., and Anderson, R. B., *J. Catal.* **68,** 339 (1981).
10. Gregg, S. J., and Sing, K. S. W., "Adsorption, Surface Area, and Porosity," p. 165. Academic Press, New York, 1978.
11. Freel, J., Robertson, S. D., and Anderson, R. B., *J. Catal.* **18,** 243 (1970).
12. Heiszman, J., Bekassy, S., and Petro, J., "Proceedings, 4th International Conference Thermal Analysis, 1974" (Buzas, I., Ed.), p. 193, Heyden Publ. Co., London, 1975.
13. Lidorenko, N. S., Kagan, A. S., Kagan, N. M., Ul'yanova, G. D., and Shishkina, A. B., *Dokl. Akad. Nauk SSSR* **197,** 154 (1971).
14. Mars, P., Scholten, J. J. F., and Zweitering, P., "Proceedings, International Congress on Catalysis, Paris, 1960," **1,** p. 1245.
15. Robertson, S. D., and Anderson, R. B., *J. Catal.* **23,** 286 (1971).
16. Nishimura, S., and Urushibara, Y., *J. Chem. Soc. Jpn.* **30,** 199 (1957).
17. Lippens, B. C., and De Boer, J. H., *J. Catal.* **3,** 44 (1964).